Uniosun Journal of Engineering and Environmental Sciences (UJEES), Vol. 8 No. 2, Sept., 2026
DOI: 10.64980/ujees.v8i2.036 **Oyewale et al.**
Published: September 30, 2026

COMPARATIVE ANALYSIS OF MACHINE LEARNING MODELS FOR ESTIMATING STEAM TURBINE ROTOR VIBRATION USING OPERATIONAL DATA FROM A NIGERIAN THERMAL POWER PLANT

O. J. OYEWALE[1*], A. A. OLAWUYI[2], M. B. OJUOLA[3], A. A. ABDULAFEEZ[4], T. O. AJEWOLE[5]

[1,2,3,4,5]*Department of Electrical and Electronic Engineering, Osun State University, Osogbo, Nigeria*

[*]*Corresponding Author: gbengajob@yahoo.com*

Abstract
Steam turbine rotor vibration is an important condition indicator for rotating machinery in thermal power plants. This study compares Artificial Neural Network (ANN), k-Nearest Neighbours (KNN), Support Vector Machine (SVM), and Decision Tree (DT) regression models for contemporaneous estimation of a composite rotor vibration index from supervisory control and data acquisition records obtained from one steam turbine unit at Egbin Thermal Power Plant, Nigeria. The raw export contained 988 records collected from 1 January to 24 March 2021 at a nominal two-hour interval. After explicit data-quality checks and removal of low-load records, 929 observations were retained. The target was the root mean square of six vibration channels, while active power, reactive power, rotor temperature, and stator core temperature were used as predictors. Data were partitioned into training, validation, and held-out test subsets before z-score scaling, and all scaling parameters and the elevated-vibration screening threshold were derived without using the test set. On the held-out test set, KNN obtained the highest regression coefficient of determination (R^2 = 0.720) and the lowest RMSE (0.00365), followed by DT (R^2 = 0.673), ANN (R^2 = 0.669), and SVM (R^2 = 0.647). For the secondary elevated-vibration screening analysis, DT achieved the highest accuracy (0.950) and F1-score (0.829), while all four models produced AUC values between 0.926 and 0.939. These results support the use of data-driven models for rotor condition monitoring, while the single-unit dataset, zero-hour prediction horizon, and absence of plant sensor-location metadata limit claims about failure prevention, generalisability, and standards-based vibration severity.

Keywords
Steam turbine; rotor vibration; machine learning; condition monitoring; predictive maintenance; rotating machinery; SCADA

1. INTRODUCTION

Nigeria has relied on a mix of thermal and hydroelectric generation as its electricity infrastructure has evolved, with thermal generating stations remaining important to grid supply [1]. Reliable operation of steam turbine-generator units is therefore important for plant availability and maintenance planning.

Steam turbine rotors and blades operate under combined thermal, mechanical, and aerodynamic loading. Shaft cracks, blade damage, thermal distortion, rotor imbalance, misalignment, bearing deterioration, and changes in condenser or steam conditions can alter vibration behaviour [2]-[9]. Vibration monitoring is consequently a widely used condition-monitoring tool for rotating machinery, but threshold alarms alone do not quantify the relationships between vibration and changing electrical or thermal operating states.

Data-driven machine learning provides a complementary approach because nonlinear relationships can be estimated directly from operational measurements [10]. Machine learning has been applied to predictive maintenance of thermal power-plant components [11], gas-turbine fault detection [12], fatigue-crack estimation [13], turbofan condition prediction [14], turbine-blade life assessment [15], and blade-crack diagnosis [16]. These studies show the value of supervised learning but also highlight the need for transparent data preparation, explicit validation, reproducible hyperparameters, and careful distinction between condition estimation and true time-ahead forecasting.

Published work using real Nigerian steam-turbine SCADA records remains limited. A previous Nigerian study examined intelligent predictive maintenance using condenser vacuum [11], but there is comparatively little published evidence comparing several classical machine-learning models for rotor vibration using operational measurements from a Nigerian thermal power plant. The present study addresses that gap using a single-unit dataset from Egbin Thermal Power Plant.

The objective is to compare ANN, KNN, SVM, and DT models for estimating a composite rotor vibration index from four contemporaneous operating variables. The study also evaluates whether the continuous model outputs can provide a secondary data-derived screening indicator for elevated vibration. The study does not claim time-ahead fault forecasting, remaining useful life estimation, or demonstrated reductions in outages.

2. MATERIALS AND METHOD

2.1. Study Area and Data Source

The operational dataset was obtained from one steam turbine unit at Egbin Thermal Power Plant, Lagos, Nigeria. The supplied file is labelled "Unit32 Vibration Data.csv" and is treated as a single-unit dataset. The raw export contains 988 records spanning 1 January 2021 13:01 to 24 March 2021 23:01. The nominal SCADA sampling interval is two hours. Across the raw timestamp sequence, 977 consecutive intervals are exactly two hours, five are four hours, one is 1 h 59 min, one is 2 h 1 min, and three duplicate timestamps occur. Six timestamps are absent from the nominal two-hour grid. One of the duplicate records is an exact row duplicate. No missing numeric values occur in the predictors or six vibration channels.

The four predictors are Active Power (MW), Reactive Power (MVAR), Rotor Temperature, and Stator Core Temperature. Rotor vibration is represented by six channels labelled Vibration 1 through Vibration 6 in the source export. The export does not contain the physical probe locations or the engineering unit of the vibration channels. These details are therefore not inferred in this manuscript. This metadata limitation prevents direct comparison of the composite index against manufacturer or ISO vibration alarm limits and should be resolved from plant instrumentation records if those records are available.

Table 1. Characteristics of the cleaned analytical dataset.

Variable	Unit	Sensor/source	Interval	N	Min	Max	Mean	SD
Active Power	MW	SCADA electrical measurement	2 h	929	39.57	216.42	180.78	36.81
Reactive Power	MVAR	SCADA electrical measurement	2 h	929	-2.77	101.68	55.87	15.11
Rotor Temperature	°C	SCADA temperature channel	2 h	929	0.36	115.07	55.16	13.68
Stator Core Temperature	°C	SCADA temperature channel	2 h	929	44.80	83.90	62.27	6.49
Vibration 1	Source unit not encoded	SCADA vibration channel V1	2 h	929	0.0010	0.0054	0.0017	0.0004
Vibration 2	Source unit not encoded	SCADA vibration channel V2	2 h	929	0.0018	0.0063	0.0046	0.0008
Vibration 3	Source unit not encoded	SCADA vibration channel V3	2 h	929	0.0221	0.0495	0.0338	0.0036
Vibration 4	Source unit not encoded	SCADA vibration channel V4	2 h	929	0.0034	0.0259	0.0155	0.0052
Vibration 5	Source unit not encoded	SCADA vibration channel V5	2 h	929	0.0443	0.1290	0.0850	0.0160
Vibration 6	Source unit not encoded	SCADA vibration channel V6	2 h	929	0.0616	0.1255	0.1015	0.0129
Composite vibration index	Same source unit as vibration channels	RMS of V1-V6	2 h	929	0.03460	0.07233	0.05640	0.00727

2.2 Data Quality Control and Preprocessing

Data quality control distinguished data-export or sensor errors from genuine elevated vibration. No generic three-standard-deviation trimming rule was applied to the composite vibration target. First, one exact duplicate row was removed. Second, 47 records with active power below 26 MW were excluded to remove off-line or very-low-load operation. This is described as a loaded-operation filter rather than a strict steady-state criterion because substantial load changes remain in the retained data. Third, seven negative rotor-temperature values were excluded as physically implausible for a loaded steam turbine. Finally, four records on 13 February 2021 were excluded after a channel-consistency check because Vibration 3 alone jumped to 0.326-0.327 while the other five vibration channels and operating variables remained comparatively stable. This signature was treated as a channel-specific sensor or data-logging error. No other high-vibration record was removed. The final analytical dataset contained 929 observations.

No imputation was required because the supplied numeric variables contain no missing values. The cleaned observations were assigned to training, validation, and test partitions in the proportions 70%, 15%, and 15%, giving 650, 139, and 140 samples, respectively. A fixed split assignment is archived with the analysis code. Importantly, the split was performed before any data-derived normalization. Z-score parameters were fitted using only the training predictors and then applied unchanged to validation and test predictors.

2.3 Prediction Horizon and Input-Target Relationship

The prediction horizon is 0 h. Each input vector and its vibration target come from the same SCADA timestamp. The models therefore estimate contemporaneous rotor vibration from the operating state; they do not forecast the next SCADA observation or vibration several minutes or hours into the future. The terms "short-term prediction" and "forecasting" have consequently been removed from the revised manuscript. Time-ahead forecasting would require lagged predictors and a future target and is reserved for future work.

2.4 Composite Rotor Vibration Index

Six vibration channels are available in each retained SCADA record. A single continuous response variable was formed using the root mean square of the simultaneous vibration measurements:

$$V_RMS = \mathrm{sqrt}[(1/n)\,\Sigma(i=1 \text{ to } n)\, V_i^2], \quad n = 6. \tag{1}$$

where V_i is the reading from vibration channel i and V_RMS is the composite vibration index. Because all six channels are combined in the same units, the composite index inherits the engineering unit of the source vibration channels. That engineering unit is not encoded in the supplied export.

2.5 Machine Learning Models and Hyperparameter Selection

All four algorithms were trained on the same four standardized predictors. Hyperparameters were selected only by performance on the validation partition, using validation R^2 as the selection criterion. The held-out test set was not used for model selection.

2.5.1 Artificial neural network

The ANN is a single-hidden-layer feedforward regression network with hyperbolic tangent hidden activation and a linear output. Candidate hidden-layer sizes were 5, 10, 15, and 20 neurons; 10 neurons produced the highest validation R^2 in the validation analysis. The MATLAB implementation uses Levenberg-Marquardt backpropagation (trainlm), a maximum of 500 epochs, and no explicit regularisation term. A fixed learning rate is not applicable to trainlm because the algorithm adapts its damping parameter during optimisation. The external validation partition is used for architecture selection and is not used to update network weights.

2.5.2 k-Nearest neighbours

KNN regression was evaluated with k values of 3, 5, 7, 9, 11, 15, and 21 and with uniform or inverse-distance weighting. Euclidean distance was used throughout. The selected configuration was k = 15 with inverse-distance weighting.

2.5.3 Support vector machine

Support vector regression used a radial basis function kernel. Candidate values were C = {0.1, 1, 10, 100}, epsilon = {0.001, 0.005, 0.01}, and gamma = {0.01, 0.1, 0.5, 1, 2}. The selected configuration was C = 0.1, epsilon = 0.001, and gamma = 2, corresponding to MATLAB KernelScale = 0.5.

2.5.4 Decision tree

The regression tree used squared-error splits. Candidate minimum leaf sizes were 2, 3, 5, 10, and 20, and candidate maximum split counts were 10, 25, 50, and 100. The selected tree used MinLeafSize = 3 and MaxNumSplits = 50. These constraints act as pre-pruning controls to limit tree complexity.

2.6 Elevated-Vibration Screening Procedure

The primary task is continuous regression. Classification metrics are reported only as a secondary screening analysis. No separate classification model was trained. Instead, the measured composite vibration index and each model's continuous prediction were converted into baseline and elevated classes using a threshold derived exclusively from the training target distribution:

$T = \text{mean}(Y_train) + SD(Y_train) = 0.063845.$ (2)

Table 2. Hyperparameter search space and selected configuration.

Model	Search space	Selected	Implementation detail
ANN	Hidden neurons: 5, 10, 15, 20	10 neurons	tanh hidden; linear output; trainlm; 500 epoch cap
KNN	k: 3, 5, 7, 9, 11, 15, 21; uniform or inverse-distance	k=15; inverse-distance	Euclidean distance
SVM	C: 0.1, 1, 10, 100; epsilon: 0.001, 0.005, 0.01; gamma: 0.01, 0.1, 0.5, 1, 2	C=0.1; epsilon=0.001; gamma=2	RBF kernel; KernelScale=0.5
Decision Tree	MinLeafSize: 2, 3, 5, 10, 20; MaxNumSplits: 10, 25, 50, 100	MinLeafSize=3; MaxNumSplits=50	Squared-error regression tree

Values below T were labelled baseline and values at or above T were labelled elevated. The training, validation, and test partitions contained 140/510, 29/110, and 21/119 elevated/baseline observations, respectively. This threshold is a data-derived screening criterion and is not presented as an ISO, manufacturer, or plant alarm limit. A standards-based threshold cannot be justified from the supplied export because the vibration engineering units and probe locations are unavailable.

2.7 Performance Evaluation

Regression performance was quantified using the coefficient of determination and root mean square error:

$R^2 = 1 - [\Sigma(y_i - \hat{y}_i)^2 / \Sigma(y_i - \bar{y})^2].$ (3)

$RMSE = \text{sqrt}[(1/N)\ \Sigma(y_i - \hat{y}_i)^2].$ (4)

Classification performance on the held-out test set was summarized using Accuracy, Precision, Sensitivity, Specificity, F1-score, Cohen's Kappa, and the Area Under the Receiver Operating Characteristic Curve (AUC). Receiver operating characteristic curves used the continuous model predictions as scores rather than the binary decisions. Residual distributions and actual-versus-predicted scatter plots were also examined.

2.8 Software, Computational Benchmark, and Code Availability

The study workflow is implemented in MATLAB using functions from the Deep Learning Toolbox and Statistics and Machine Learning Toolbox. The source project did not record the MATLAB release number, so no version number is inferred. The analysis code records model-training time and per-sample prediction time and exports all model metrics. Absolute timing depends on hardware and software implementation, so the reported benchmark is interpreted comparatively. The MATLAB code is provided with the submission package. Availability of the plant SCADA data outside the submission package is subject to plant data-sharing permission.

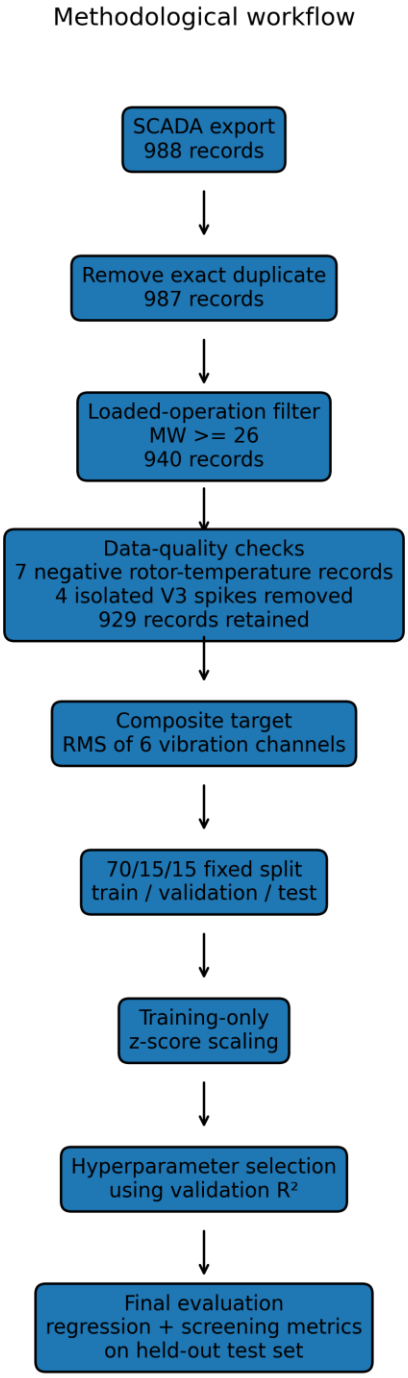


Figure 1. Methodological workflow from SCADA data quality control to held-out model evaluation.

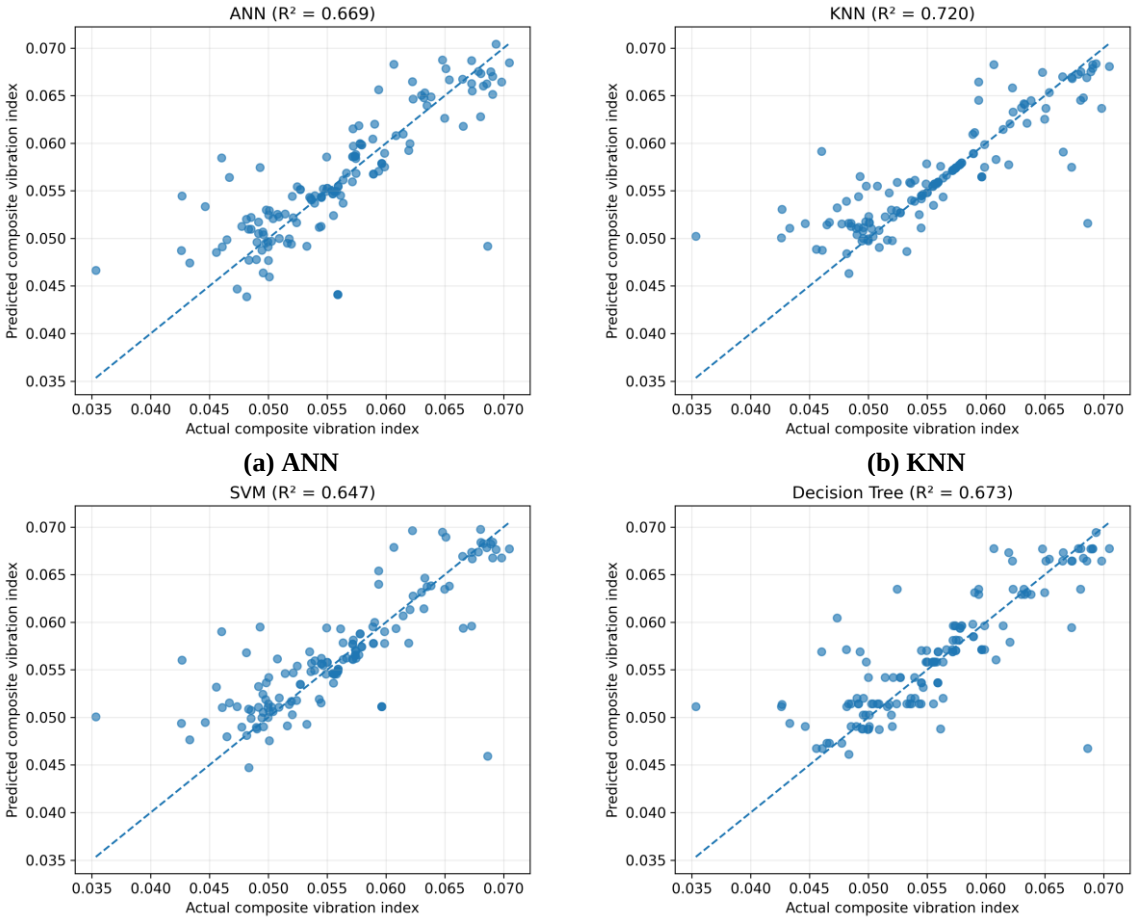
3. RESULTS AND DISCUSSION

3.1 Regression Performance

KNN achieved the highest test R^2 (0.720) and the lowest test RMSE (0.00365), indicating the best continuous-estimation performance among the four models. DT ranked second by test R^2 (0.673), closely followed by ANN (0.669), while SVM obtained a test R^2 of 0.647. The validation and test values are lower than the corresponding training values for every model, which is expected when performance is assessed on unseen samples. The near-unity in-sample KNN R^2 is characteristic of distance-weighted KNN when training observations can retrieve themselves and should not be interpreted as evidence of superior generalisability. Model comparison is therefore based primarily on validation and held-out test performance.

Table 3. Regression performance across training, validation, and held-out test partitions.

Model	Train R^2	Val R^2	Test R^2	Train RMSE	Val RMSE	Test RMSE
ANN	0.840	0.772	0.669	0.00293	0.00350	0.00397
KNN	1.000	0.772	0.720	0.00011	0.00350	0.00365
SVM	0.922	0.724	0.647	0.00204	0.00385	0.00410
Decision Tree	0.873	0.638	0.673	0.00261	0.00441	0.00395



(a) ANN **(b) KNN**

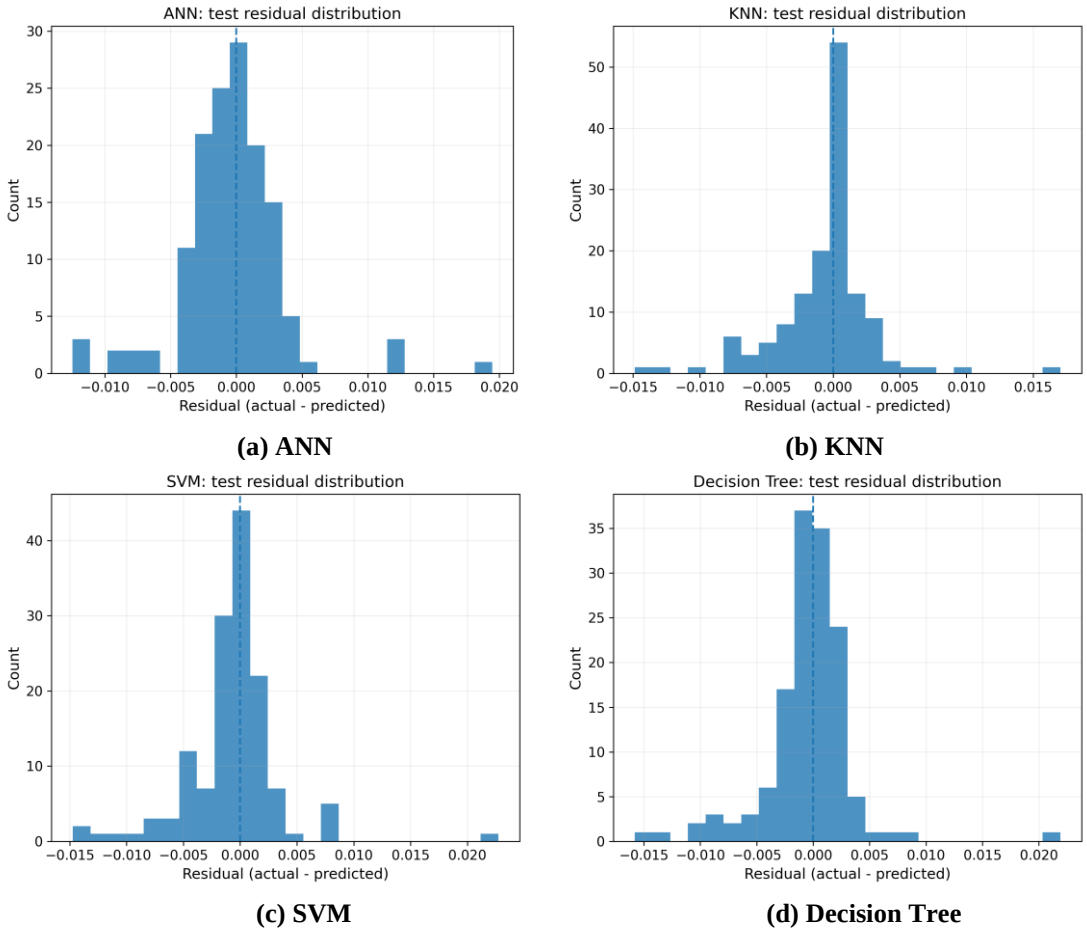
(c) SVM **(d) Decision Tree**

Figure 2. Actual versus predicted composite vibration index on the held-out test set. The dashed line in each panel represents ideal agreement.

The scatter plots in Figure 2 show that KNN follows the one-to-one line most consistently across the central operating region. ANN and DT also track the measured index reasonably well, while SVM shows somewhat greater shrinkage toward the centre of the response range. The models are estimating the same-time vibration index, so these plots should not be interpreted as time-ahead forecasts.

3.2 Residual Analysis

Residual means were small for all models, ranging in magnitude from approximately 0.00031 to 0.00066. The corresponding residual standard deviations were approximately 0.0036 to 0.0041. This indicates limited overall bias, although the spread of residuals confirms that none of the models reproduces every vibration observation exactly. Residual analysis therefore supports the use of the models for condition estimation but not deterministic fault declaration.



(a) ANN **(b) KNN**

(c) SVM **(d) Decision Tree**

Figure 3. Residual distributions for the four models on the held-out test set.

3.3 Elevated-Vibration Screening Performance

DT achieved the highest test classification accuracy (0.950), F1-score (0.829), Kappa (0.800), and specificity (0.975). ANN achieved sensitivity of 0.810 and the highest AUC (0.939). KNN and SVM also produced AUC values above 0.92. These metrics describe discrimination relative to the training-derived statistical threshold and should not be interpreted as proof that the models detect engineering faults or predict failure events.

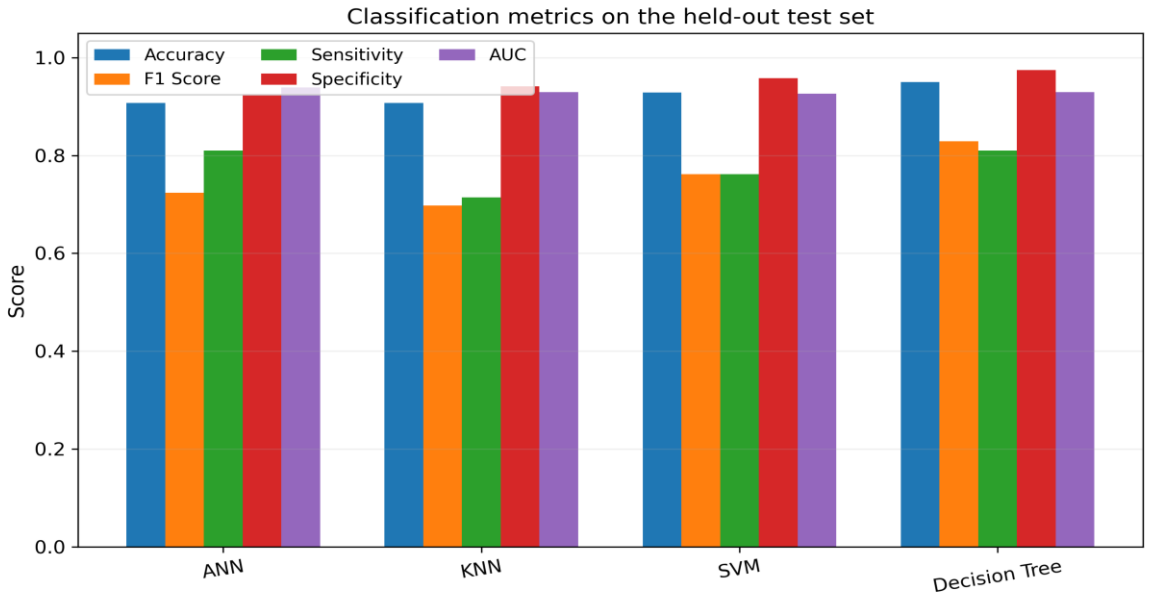


Figure 4. Classification metrics for all four models using the same held-out test set and the same training-derived screening threshold.

Table 4. Classification metrics for baseline versus elevated vibration on the held-out test set.

Model	Accuracy	Precision	Sensitivity	Specificity	F1-score	Kappa	AUC
ANN	0.907	0.654	0.810	0.924	0.723	0.668	0.939
KNN	0.907	0.682	0.714	0.941	0.698	0.643	0.929
SVM	0.929	0.762	0.762	0.958	0.762	0.720	0.926
Decision Tree	0.950	0.850	0.810	0.975	0.829	0.800	0.929

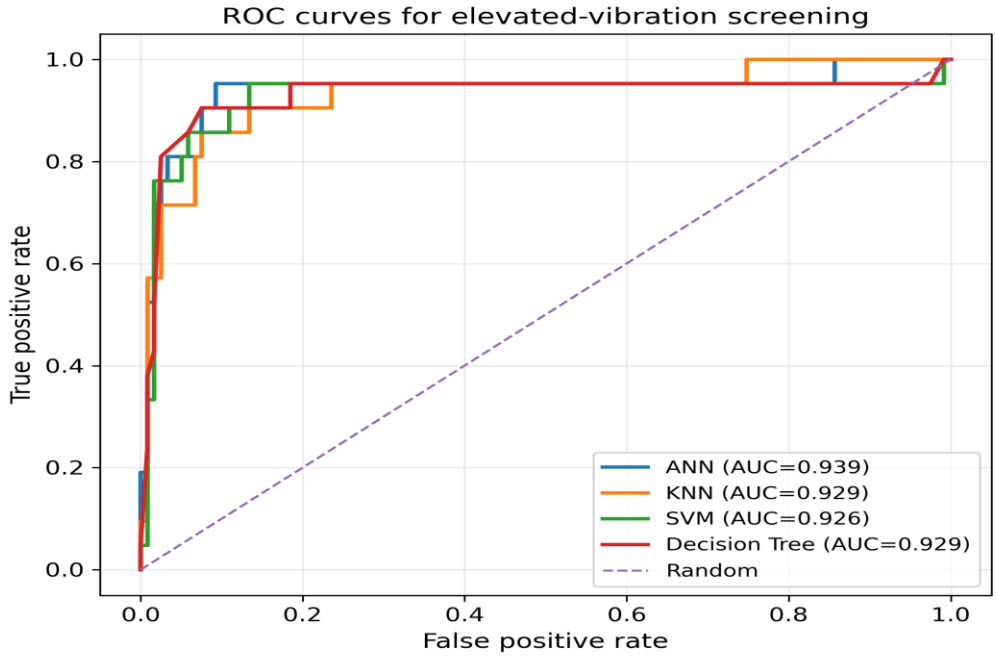


Figure 5. Receiver operating characteristic curves for elevated-vibration screening. AUC values are based on continuous predicted vibration scores.

3.4 Decision Tree Interpretability

The Decision Tree provides a transparent sequence of operating-state splits that can be inspected by maintenance engineers. In the selected tree, rotor temperature had the largest normalized importance (approximately 0.466), followed by active power (0.244), reactive power (0.168), and stator core temperature (0.122). These values are model-specific importance measures, not causal effects. Their practical value is that a tree can expose which operating variables are most frequently used to partition higher and lower vibration states, making it easier to review model behaviour against engineering experience.

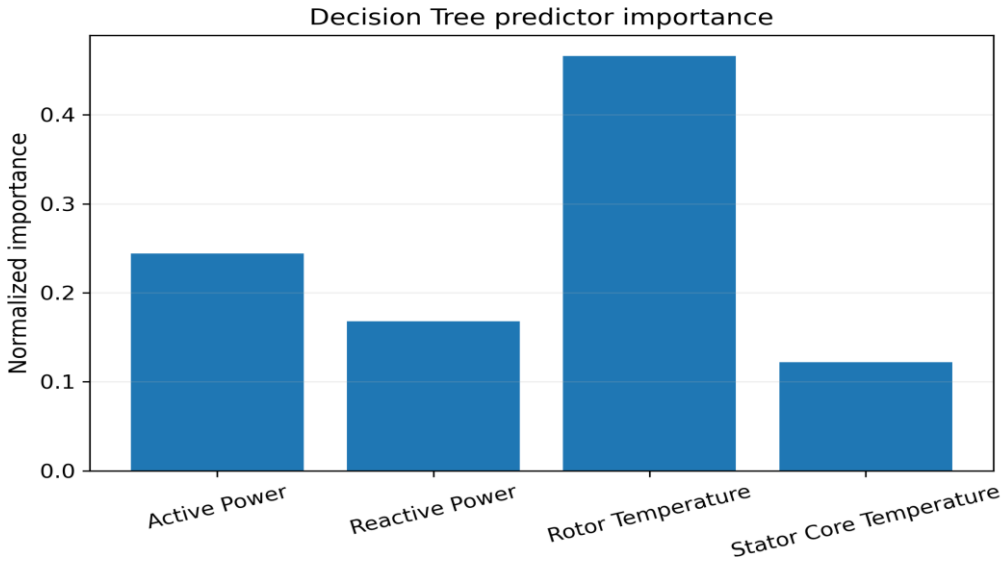


Figure 6. Normalized predictor importance from the selected Decision Tree model.

3.5 Computational Cost and Practical Deployment

The measured inference times are negligible relative to the nominal two-hour SCADA interval. This suggests that computational throughput is unlikely to be the main barrier to online deployment. More important practical issues are reliable sensor metadata, handling of missing or invalid SCADA records, model drift as operating regimes change, controlled retraining, integration with existing historian or condition-monitoring infrastructure, and cyber-security requirements. A deployed system should also retain conventional protection and alarm functions rather than replace them with a statistical model.

Table 5. Reference computational benchmark. Absolute values are hardware- and implementation-dependent.

Model	Training time (ms)	Prediction time per sample (µs)
ANN	522.64	0.54
KNN	0.31	4.80
SVM	10.49	7.89
Decision Tree	1.79	0.24

3.6 Discussion and Limitations

The results show that no single model dominates every metric. KNN provided the best held-out continuous regression performance, whereas DT provided the strongest threshold-based screening metrics and the clearest interpretability. ANN and SVM remained competitive, particularly in AUC. This pattern is consistent with the broader literature showing that algorithm suitability depends strongly on data distribution, operating regime, validation design, and the chosen performance objective [10]-[14].

The study has several important limitations. First, the dataset covers one turbine unit and one operating period, so the results do not establish generalisability to other units or plants. Second, the supplied export does not contain the physical locations or engineering units of the six vibration channels, which prevents standards-based vibration severity classification. Third, the prediction horizon is zero hours; the study estimates current vibration and does not forecast future failure, remaining useful life, or maintenance outcomes. Fourth, the randomized holdout design is suitable for evaluating interpolation across observed operating states but does not reproduce a future chronological deployment scenario and may retain temporal dependence between nearby records. Future work should therefore use a separate later operating period and, ideally, external validation on another turbine or plant.

Accordingly, the findings demonstrate potential for data-driven condition monitoring. They do not demonstrate that the models themselves reduce failures, maintenance costs, or unplanned outages. Such claims would require a prospective deployment study linking model alerts to verified maintenance decisions and operational outcomes.

4. CONCLUSION

This study compared ANN, KNN, SVM, and DT models for contemporaneous estimation of a six-channel RMS steam-turbine rotor vibration index from four SCADA operating variables. The analysis used explicit data-quality checks, training-only normalization parameters, validation-based hyperparameter selection, a held-out test set, and a training-derived threshold for the secondary elevated-vibration screening analysis.

On the held-out test set, KNN produced the strongest regression result with $R^2 = 0.720$ and RMSE = 0.00365. DT achieved the strongest secondary screening performance with accuracy = 0.950 and F1-score = 0.829, while ANN achieved the highest AUC of 0.939. These results indicate that classical machine-learning models can provide useful estimates of rotor vibration condition from operational data, but model selection depends on whether continuous estimation, class discrimination, or interpretability is the primary objective.

Future work should obtain complete vibration-probe metadata and engineering units; validate thresholds against manufacturer or applicable standards; evaluate lagged time-ahead forecasting; use chronological and external validation datasets; include additional measurements such as bearing temperature, lubrication condition, steam pressure, steam flow, and shaft displacement; investigate drift detection and periodic retraining; and prospectively assess whether model-assisted decisions improve maintenance outcomes.

REFERENCES

[1] N. Edomah, C. Foulds, and A. Jones, "Energy Transitions in Nigeria: The Evolution of Energy Infrastructure Provision (1800-2015)," Energies, vol. 9, no. 7, art. 484, 2016, doi: 10.3390/en9070484.

[2] A. Bovsunovsky, E. Shtefan, and V. Peshko, "Modeling of the circumferential crack growth under torsional vibrations of steam turbine shafting," Theoretical and Applied Fracture Mechanics, vol. 125, art. 103881, 2023, doi: 10.1016/j.tafmec.2023.103881.

[3] N. Omenife, D. Desai, and R. Dunne, "Transient Analysis of Thermal Bending and Vibration of Steam Turbine Rotor," Science, Engineering and Technology, vol. 3, no. 2, pp. 84-96, 2023, doi: 10.54327/set2023/v3.i2.91.

[4] Z. Ali, Z. Abbas, and S. Abbas, "Investigation of High Vibration Phenomena in Steam Turbine: An Experimental Exploration into Root Causes and Material Analysis," Advanced Materials & Sustainable Manufacturing, vol. 1, no. 2, art. 10007, 2024, doi: 10.35534/amsm.2024.10007.

[5] W. M. Ashraf et al., "Artificial intelligence based operational strategy development and implementation for vibration reduction of a supercritical steam turbine shaft bearing," Alexandria Engineering Journal, vol. 61, no. 3, pp. 1864-1880, 2022, doi: 10.1016/j.aej.2021.07.039.

[6] D. M. Graciano, J. A. Rodríguez, G. Urquiza, and M. Tecpoyotl-Torres, "Damage evaluation and life assessment of steam turbine blades," Theoretical and Applied Fracture Mechanics, vol. 124, art. 103782, 2023, doi: 10.1016/j.tafmec.2023.103782.

[7] Y. Kaneko, "Mechanical design and vibration analysis of steam turbine blades," in Advances in Steam Turbines for Modern Power Plants, 2nd ed., Elsevier, 2022, pp. 139-162, doi: 10.1016/B978-0-12-824359-6.00007-X.

[8] R. Rzadkowski, P. Troka, J. Manerowski, L. Kubitz, and M. Kowalski, "Nonsynchronous Rotor Blade Vibrations in Last Stage of 380 MW LP Steam Turbine at Various Condenser Pressures," Applied Sciences, vol. 12, no. 10, art. 4884, 2022, doi: 10.3390/app12104884.

[9] P. Hu, Q. Meng, W. Fan, W. Gu, J. Wan, and Q. Li, "Vibration characteristics and life prediction of last stage blade in steam turbine based on wet steam model," Engineering Failure Analysis, vol. 159, art. 108127, 2024, doi: 10.1016/j.engfailanal.2024.108127.

[10] M. Bertolini, D. Mezzogori, M. Neroni, and F. Zammori, "Machine Learning for industrial applications: A comprehensive literature review," Expert Systems with Applications, vol. 175, art. 114820, 2021, doi: 10.1016/j.eswa.2021.114820.

[11] T. O. Ajewole, O. Onarinde, M. K. Agboola, A. O. Alao, and O. D. Momoh, "Employment of Intelligent Predictive Maintenance on Thermal Power Plant Component Parts Taking Condenser Vacuum as a Case Study," Tanzania Journal of Engineering and Technology, vol. 42, no. 3, pp. 34-47, 2023, doi: 10.52339/tjet.v42i3.953.

[12] W. M. Salilew, Z. A. A. Karim, and T. A. Lemma, "Investigation of fault detection and isolation accuracy of different machine learning techniques with different data processing methods for gas turbine," Alexandria Engineering Journal, vol. 61, no. 12, pp. 12635-12651, 2022, doi: 10.1016/j.aej.2022.06.026.

[13] M. Badora, M. Sepe, M. Bielecki, A. Graziano, and T. Szolc, "Predicting length of fatigue cracks by means of machine learning algorithms in the small-data regime," Eksploatacja i Niezawodność - Maintenance and Reliability, vol. 23, no. 3, pp. 575-585, 2021, doi: 10.17531/ein.2021.3.19.

[14] M. Matuszczak, M. Żbikowski, and A. Teodorczyk, "Predictive modelling of turbofan engine components condition using machine and deep learning methods," Eksploatacja i Niezawodność - Maintenance and Reliability, vol. 23, no. 2, pp. 359-370, 2021, doi: 10.17531/ein.2021.2.16.

[15] B. Vasilyev, S. Nikolaev, M. Raevskiy, S. Belov, and I. Uzhinsky, "Residual Life Prediction of Gas-Engine Turbine Blades Based on Damage Surrogate-Assisted Modeling," Applied Sciences, vol. 10, no. 23, art. 8541, 2020, doi: 10.3390/app10238541.

[16] G. Zhu, C. Wang, W. Zhao, Y. Xie, D. Guo, and D. Zhang, "Blade Crack Diagnosis Based on Blade Tip Timing and Convolution Neural Networks," Applied Sciences, vol. 13, no. 2, art. 1102, 2023, doi: 10.3390/app13021102.